AIP Advances

RESEARCH ARTICLE | JUNE 07 2024

Diagnostic neutral beam injector for active spectroscopy of high beta plasmas

N. Stupishin ; V. Belov ; A. Brul ; V. Davydenko ; P. Deichuli ; A. Kolmogorov ; V. Kolmogorov; V. Oreshonok ; R. Vakhrushev; D. Osin

Check for updates

AIP Advances 14, 065314 (2024)
https://doi.org/10.1063/5.0203708

View Online
Export Citation

26 June 2024 06:54:28


APL Energy
Latest Articles Online!
Read Now
AIP Publishing

AIP Publishing

Diagnostic neutral beam injector for active spectroscopy of high beta plasmas

Cite as: AIP Advances 14, 065314 (2024); doi: 10.1063/5.0203708
Submitted: 22 February 2024 • Accepted: 20 May 2024 •
Published Online: 7 June 2024

View Online Export Citation CrossMark

N. Stupishin,[1,a)] V. Belov,[1] A. Brul,[1] V. Davydenko,[1] P. Deichuli,[1] A. Kolmogorov,[1] V. Kolmogorov,[1] V. Oreshonok,[1] R. Vakhrushev,[1] and D. Osin[2]

AFFILIATIONS

[1] Budker Institute of Nuclear Physics, Novosibirsk, Russia
[2] Tokamak Energy Ltd., Abingdon, United Kingdom

[a)] **Author to whom correspondence should be addressed:** n.v.stupishin@inp.nsk.su

ABSTRACT

The advanced fast ion-dominated high beta plasma is achieved using multi-MW neutral heating beams. To facilitate the diagnostics of this fast ion-dominated plasma, a high-energy and high-current diagnostic neutral beam (DNB) injector was designed and built by the Budker Institute of Nuclear Physics. The DNB injector made active measurements of ion temperature and rotational velocity possible with the help of charge-exchange spectroscopy for impurity ions and, most importantly, for the main ion (deuterium) component. A DNB energy of 40 keV was chosen to assure low beam attenuation in the plasma and to enable spectroscopic measurements along the entire plasma column. The diameter (level 1/e) of the ballistically focused DNB in the plasma is about 8 cm. To achieve a high temporal resolution, unique methods of beam modulation with a frequency of up to 10 kHz were implemented. The achieved high DNB current of 8 A in atomic hydrogen in combination with the beam modulation enables to obtain an acceptable signal-to-noise ratio of the measured spectra.

© 2024 Author(s). All article content, except where otherwise noted, is licensed under a Creative Commons Attribution-NonCommercial-NoDerivs 4.0 International (CC BY-NC-ND) license (https://creativecommons.org/licenses/by-nc-nd/4.0/). https://doi.org/10.1063/5.0203708

26 June 2024 06:54:28

I. INTRODUCTION

High beta plasmas are often driven in gas dynamic traps,[1] reversed field pinches, field reversed configurations (FRCs), and spherical tokamaks by multi-MW neutral heating beams, and thus, the fast ion population in the plasma is significant. Measurements of the key plasma parameters, such as ion temperature and velocity of rotation, are strongly affected by the presence of high-energy ions. Diagnostic neutral beams play a crucial role in active plasma spectroscopy and are widely used in almost all fusion-related experiments for reliable measurement of the ion density and temperature, electron density fluctuations, fast ion velocity distribution function, and magnetic field.[2–6] Due to the high intensity background of fast ions in the plasma, the requirements of the DNB injector parameters are quite challenging. Hence, the demand for high spatial resolution and a high signal-to-noise ratio results in high beam current density and low beam divergence. In order to make measurements across the entire plasma column, the beam energy should be high enough that the beam attenuation is insignificant. This, in turn, sets a high limit on the beam main energy fraction. In addition, the beam main ion species energy should be higher than that of the background fast ions produced by the powerful heating neutral beams (HNBs) to allow one to distinguish between the contribution of the DNB and that of HNBs to the observed spectra. It is always desired to follow the plasma dynamics throughout the discharge lifetime and to have the highest temporal resolution. To satisfy these requirements, the DNB pulse duration should span the entire plasma lifetime and the beam should be modulated. The DNB modulation frequency has to be higher than the rate of the characteristic plasma parameter changes. The high DNB modulation frequency results in a short integration time of the measurement, which, again, demands a high beam current density, as mentioned above. The main requirements of the DNB are listed in Table I.

Based on these requirements, a state-of-the-art DNB injector was designed and built at the Budker Institute of Nuclear Physics. In this paper, a general description of the DNB injector is given and the main parts of the injector are described in detail.

II. DESCRIPTION OF THE DNB INJECTOR

The principle of operation of a neutral beam injector is in brief described below. Prior to neutral beam injection, a plasma dis-

© Author(s) 2024

TABLE I. Main parameters of the diagnostics neutral beam.

1	Beam particles	Hydrogen /deuterium
2	Full energy of neutrals	up to 43 keV
3	Full energy fraction	>80%
4	Maximum oxygen/carbon fraction	0.5%
5	Beam radius at focus (at the e-fold level)	4 cm
6	Focal distance of the ion optics system	≈3 m
7	Beam angular divergence	<15 mrad
8	Total neutral beam current	>8 A
9	Total ion beam current	>15 A
10	Maximum beam modulation frequency	10 kHz
11	Modulation depth of the beam current at focus	>60%
12	Minimum flat top duration	25 μs
13	Maximum flat top change	5%
14	Pulse duration	30 ms
15	Pulse repetition	10 min
16	Maximum gas bleed rate	1 Torr ∗ l/s

charge is produced and maintained by a cold-cathode arc plasma generator.[6,7] To this end, a working gas (molecular hydrogen in this case) is injected into the plasma generator, and an arc discharge is ignited between the cathode and the anode of the plasma generator. The plasma thus produced expands through the anode orifice into the cylindrical chamber of the plasma source with the peripheral multipole magnetic field. The IOS with spherical electrodes extracts and forms an ion beam, which contains both atomic and molecular ions of hydrogen. When passing through the neutralizer region, the accelerated ions dissociate and are partly neutralized (the neutralization efficiency for 40 keV ions is ~62%). A bending magnet installed in the beam duct deflects ions and directs them into the ion dump. A beam of neutral atoms continues toward the target plasma in the main experimental vessel for diagnostic purposes. A schematic of the principle of operation of a neutral beam injector is shown in Fig. 1.

III. DNB INJECTOR VACUUM VESSEL

The DNB injector dimensions and placement on the FRC[8] machine were determined to a great extent by the geometry of ports,

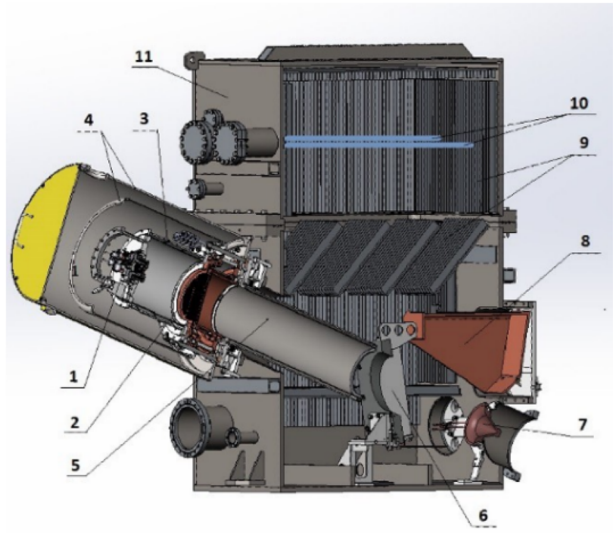

FIG. 2. 3D model of the DNB injector vacuum vessel (cross section): 1—plasma generator, 2—ion optical system, 3—plasma expander, 4—electromagnetic shielding, 5—neutralizer, 6—bending magnet, 7—movable beam collector, 8—ion beam dump, 9—finned panels, 10—titanium gettering rods, and 11—injector vacuum tank.

by the diagnostics suite, and by the heating neutral beams located on both sides of the DNB injector. These limitations led to a compact vacuum vessel and a relatively short (3 m) focal distance of the IOS. In addition, a more compact DNB injector vessel along the beam path is necessary for minimization of the beam cross section at the focal distance. A three dimensional model of the DNB injector vacuum vessel is shown in Fig. 2.

The DNB injector vessel consists of two parts in the shape of a parallelepiped. Two titanium gettering rods are installed in the top part. The beam duct is in the lower part of the vessel with dimensions of 780 × 825 × 1000 mm^3. The inner walls are equipped with finned panels to increase the pumping speed due to the increased surface of the titanium coating. The total volume of the vacuum vessel is 1 m^3. The injector axis is offset from the median plane by about 200 mm in order to fit the beam through the entrance port on the FRC vessel. The beam axis is tilted by 20.4° relative to the

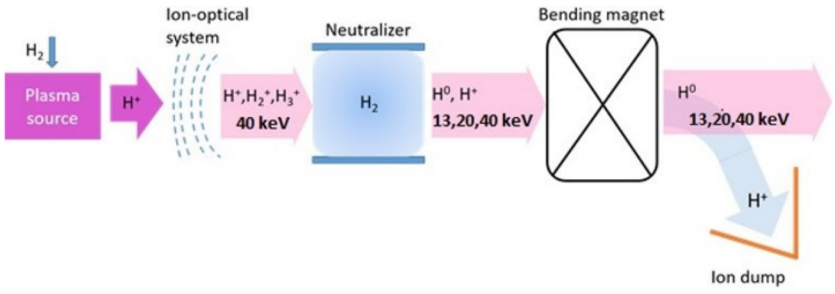

FIG. 1. Principle of operation of a neutral beam injector.

26 June 2024 06:54:28

© Author(s) 2024

horizontal plane and is perpendicular to the geometrical axis of the vessel.

IV. DNB INJECTOR PLASMA GENERATOR

The DNB injector pulse duration is equal to that of the plasma lifetime, 30 ms. Based on this parameter and on the requirements for a low concentration of molecular ions, a cold cathode arc plasma generator was chosen as the plasma source. The maximum ion beam current achieved with the single plasma generator is 15.5 A, which is high enough to meet the requirement of equivalent neutral beam current (see Table I). This arc plasma generator is analogous to that used in the heating beams made at Budker Institute and is described in great detail elsewhere.[9]

V. ION OPTICAL SYSTEM

The DNB injector ion optical system has a diameter of 180 mm and consists of four electrodes made of chromium–zirconium brass, exhibiting high mechanical strength and high thermal conductivity. The beam is formed from 943 circular apertures with a diameter of 4 mm each, which are arranged in a hexagonal pattern.

The electrodes are spherical in order to focus the beam in the plasma confinement vessel axis at a distance of 3 m from the IOS. However, due to a 10%–15% radial decrease in the emission current density, the IOS electrodes have increasing radii of curvature down the beam line. This leads to radially increasing accelerating gaps, which, in turn, results in optimized accelerating gaps that scale according to the Child–Langmuir law $d(r) \sim j(r)^{-1/2}$ along the entire radius. Thus, it is ensured that the formation of elementary beams both in central and peripheral cells is done at perveance optimum, thereby guaranteeing minimum angular divergence.

In order to estimate the optimum inter-electrode gaps, taking into account the real radii of curvature after the manufacturing process, a single cell modeling of a beam has been performed for both central and peripheral cells of the IOS. An example of the beam formation modeling in a central cell made using the PBGUNS[10] code is shown in Fig. 3.

The result of the simulations with realistic inputs was that the optimal voltage drop in the gap between the first and the second grids was found to be 14% of the full voltage.

The optimized geometrical parameters of the IOS electrodes and applied voltages are presented in Table II. Gaps between the IOS electrodes are given for both central and peripheral regions of the grid in Table II.

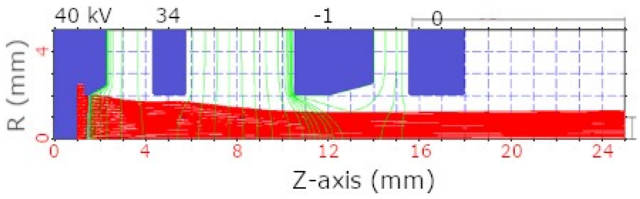

FIG. 3. Modeling of a beam formation in a central cell of the four electrode DNB injector IOS.

TABLE II. Main parameters of the DNB injector IOS electrodes.

	Grid 1	Grid 2	Grid 3	Grid 4
Thickness (mm)	2	1.5	3.5	2.5
Curvature R_c (mm)	3500	3000	2200	2200
Gap C/E (mm)		1.73/2.11	4.50/4.93	1.30/1.31
Voltage (kV)	+40.0	+34.4	−0.7	0 (ground)

VI. BEAM DUCT

The DNB injector beam duct is shown in Fig. 4.

In order to get a focused neutral beam, the IOS has to be located as close to the focal plane as possible. As was mentioned above, the size of the beam is proportional to the IOS focal distance $R_e \sim F \cdot [\alpha_{abb}{}^2 + (v_{Ti}/v_b)^2]^{1/2}$, where F is the focal distance of the IOS, α_{abb} is the beam angular divergence caused by the IOS aberrations, v_{Ti} is the thermal velocity of the beam particles, and v_b is the beam velocity. From the expression given above, one can see that a shorter focal length is beneficial for the smaller beam size.

The beam duct consists of a neutralizer, where ions are turned into atoms, a bending magnet to deflect charged particles, two collectors of deflected positive and negative ions, and a movable calorimeter for working with the beam in the test mode.

The bending magnet removes the charged particles that are not neutralized from the beam. As mentioned above, in addition to atomic ions H^+, the plasma generator produces molecular ions H^{2+} and H^{3+}. When molecular ions are passing the neutralizer, they dissociate due to collisions with the neutral gas. As a result, slower energy fractions $E_0/2$ and $E_0/3$ are formed along with the main energy component E_0. The bending magnet deflects all positive ions into a special stand-alone ion collector. The bending magnet represents a U-shaped magnetic core made of iron with large magnetic permeability. Permanent magnets NdFeB (B = 1.3 T) of a rectangular shape of 80 × 80 × 30 mm^3 are placed in the poles. The distance between the poles is 190 mm. The magnet is tilted by 30° and is shifted downward by 30 mm relative to the beam axis.

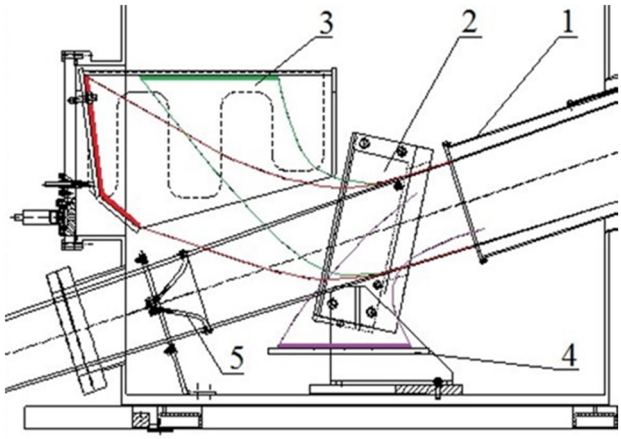

FIG. 4. DNB injector beam duct. 1—neutralizer, 2—bending magnet, 3—positive ion collector, 4—negative ion collector, and 5—movable calorimeter.

26 June 2024 06:54:28

© Author(s) 2024

The box-shaped positive ion collector is made of copper. The width of the entrance window is 200 mm. The energy absorbed by the ion collector during the 30 ms long beam pulse is about 7.5 kJ. A copper pipe is welded to the collector edges to provide water cooling of the ion collector between pulses.

The fraction of negative ions in the beam is about 1%. For this reason, they are collected on a copper plate, mounted directly on the bending magnet.

VII. BEAM MODULATION TECHNIQUES

Various methods can be employed for beam modulation.[11] In this paper, we describe unique techniques that were used to achieve a high frequency beam modulation of up to 10 kHz.

A. High voltage modulation

The DNB injector power supply allows us to modulate the full voltage (40 kV) with a frequency of up to 1 kHz. During this period, when the high voltage is off, the arc plasma generator current is switched from the upper level of around 500 A to a lower level of 360 A. This is necessary to prevent a breakdown on the rising front of the next high voltage pulse. After the high voltage is applied, the arc current is increased back to the upper level within 0.4 ms. The arc current rise time is determined by the inductive components in the arc generator power supply. They determine the maximum beam modulation frequency of about 1 kHz when this modulation technique is used. The oscillogram depicted in Fig. 5 shows traces of high voltage and beam currents when the beam is modulated at 0.5 kHz.

B. Modulation by beam defocusing

A second method of beam modulation, which was implemented on this DNB injector, is beam defocusing. As mentioned above, the optimal voltage difference in the first electrode gap should be 14% of the full beam energy. When this voltage difference is increased by 2–3 kV, the beam is significantly defocused and the beam current density at the focal plane drops by 2–2.5 times, while the beam current remains fixed. This allows us to avoid transient processes on the pulse fronts and provides a higher modulation frequency of up to 10 kHz. Such a modulation is achieved by modulating the voltage on the second grid.

The beam current profile was measured by a secondary electron emission (SEE) two-dimensional detector array, which was located 3.8 m away from the IOS. Nine conical molybdenum detectors are arranged in a cross with a period of 2.5 cm. The SEE detectors were used to measure both the beam profile and the beam angular divergence while testing the fast beam defocusing technique. The SEE detector traces for the beam modulation at 10 kHz are shown in Fig. 6.

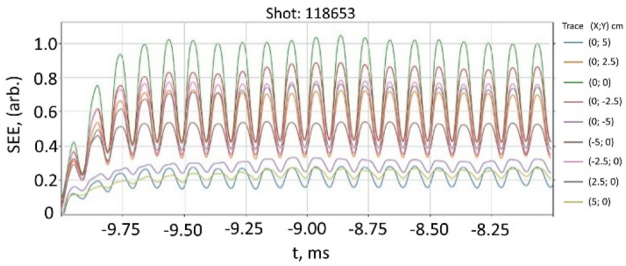

FIG. 6. Beam modulation by beam defocusing at 10 kHz recorded by the SEE detectors located at 3.8 m from the IOS. The modulation depth is 50%–70%. The beam pulse fragment of 2 ms.

C. Modulation by varying the plasma flux

The third technique of beam modulation is based on changing the plasma flux toward the IOS by fast commutation of the arc discharge current between the generator anode and the DNB injector vacuum vessel walls. It was found experimentally that commutation of 60% of the arc discharge current to the walls results in an increase in the plasma flux and a corresponding beam current increase of up to two times. The transition time from one discharge regime to another is about 65 μs, which is sufficient to achieve a beam modulation frequency of 5–7 kHz. The oscillogram depicted in Fig. 7 shows traces of high voltage and arc and beam currents when the beam is modulated at 5 kHz.

To obtain higher beam modulation frequencies, a faster stabilization of the arc current is required. This can be achieved by increasing the frequency of the arc choppers, which currently is 20 kHz.

VIII. BEAM ENERGY FRACTIONS

The beam energy fractions were determined by observing Doppler shifted Hα spectral lines emitted by the beam atoms due to collisions with the residual gas. Each spectral line corresponds to a certain beam energy component. The observed spectral lines

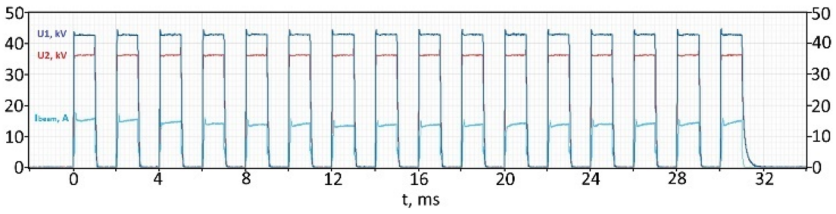

FIG. 5. Beam modulation at 0.5 kHz by means of high voltage modulation. The modulation depth is 100%.

26 June 2024 06:54:28

© Author(s) 2024

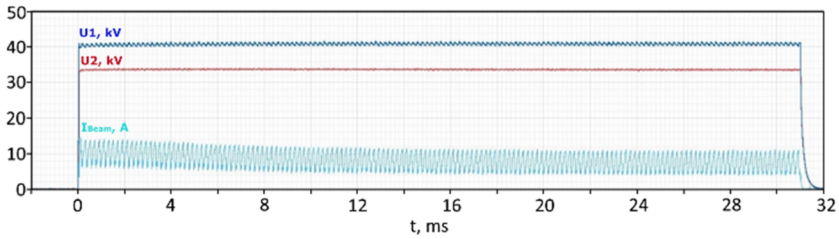

FIG. 7. Beam modulation at 5 kHz by commutating the arc current to the chamber wall and varying plasma flux on the IOS first grid. The modulation depth is 50%.

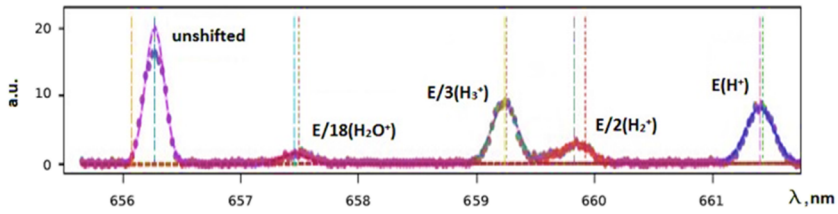

FIG. 8. DNB Doppler shifted H_α spectrum observed at 35° to the beam axis. The beam full energy is 40 kV.

were fitted with Gaussian profiles, and their intensity ratio was used to calculate the beam energy fractions.[12] The optical line of sight was at an angle of about 35° to the beam axis in order to resolve spectral lines of all energy fractions that are present in the beam. A typical Doppler shifted beam Hα spectrum is presented in Fig. 8.

The typical beam energy composition (in current) thus determined—H^+: 84.6%, H^{2+}: 6.0%, H^{3+}: 8.7%, and H^{18+}: 0.7%—fully satisfies the beam requirements, as shown in Table I.

IX. BEAM SIZE AND DIVERGENCE

The beam profile was measured with the help of the two-dimensional array of SEE detectors, located 3.8 m away from the IOS. The measured beam profile in the horizontal plane is shown in Fig. 9.

The beam size (at the e-fold level) in the focal plane was determined based on these measurements as 4.0 cm. The experimentally obtained beam angular divergence is 14 mrad. Both the beam size and the angular divergence obtained in the course of beam com-

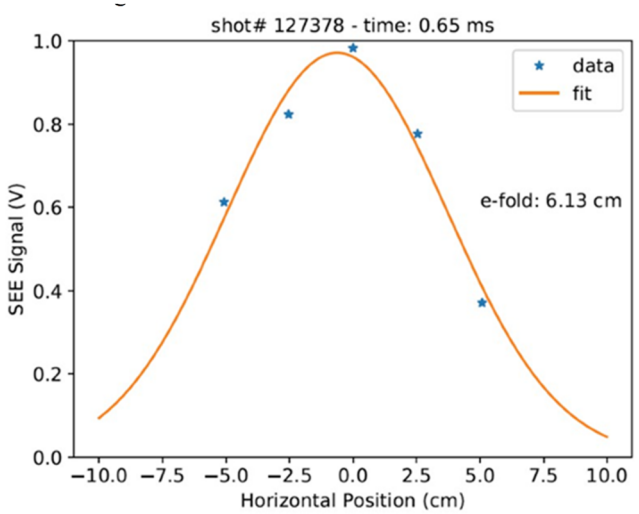

FIG. 9. DNB size and divergence as measured with the SEE detector on a test stand 3.8 m from the IOS.

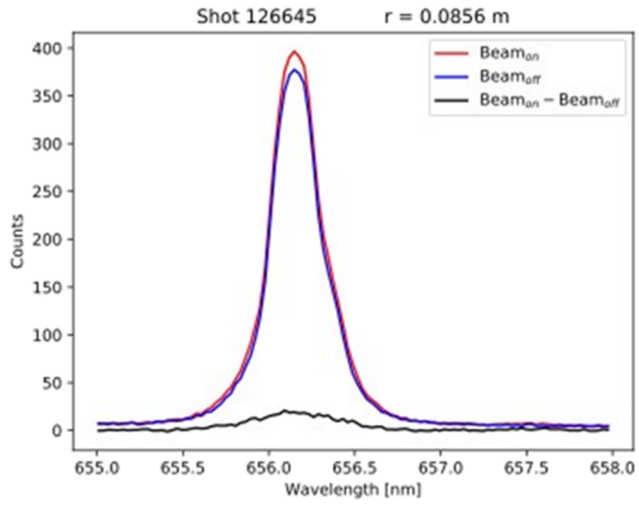

FIG. 10. Active and passive CHERS Hα spectra of the main ion at R = 9 cm from the plasma axis.

26 June 2024 06:54:28

© Author(s) 2024

missioning fully satisfy the beam requirements listed in Table I. The equivalent current density of 40 keV hydrogen atoms in the DNB focus is 150 mA/cm^2.

X. PLASMA DIAGNOSTICS WITH THE DNB INJECTOR

Since the end of 2019, the DNB injector has been extensively used for plasma diagnostics on the FRC machine.[13,14] Key plasma parameters such as main ion and impurity ion temperature and velocity of rotation are regularly measured with the help of charge-exchange recombination spectroscopy (CHERS).[2,3] A typical example of the main ion passive and active CHERS Balmer-α spectra, when the beam is off and on, respectively, is shown in Fig. 10.

The achieved DNB parameters are of paramount importance for obtaining the required accuracy of the ion temperature and rotational velocity measurements.

AUTHOR DECLARATIONS

Conflict of Interest

The authors have no conflicts to disclose.

Author Contributions

N. Stupishin: Writing – original draft (equal). **V. Belov**: Writing – original draft (equal). **A. Brul**: Writing – original draft (equal). **V. Davydenko**: Writing – original draft (equal). **P. Deichuli**: Writing – original draft (equal). **A. Kolmogorov**: Writing – original draft (equal). **V. Kolmogorov**: Writing – original draft (equal). **V. Oreshonok**: Writing – original draft (equal). **R. Vakhrushev**: Writing – original draft (equal). **D. Osin**: Writing – original draft (equal).

DATA AVAILABILITY

The data that support the findings of this study are available from the corresponding author upon reasonable request.

REFERENCES

[1]A. A. Ivanov *et al.*, "Experimental evidence of high-beta plasma confinement in an axially symmetric gas dynamic trap," Phys. Rev. Lett. **90**, 105002 (2003).
[2]J. W. Coenen *et al.*, "Charge exchange recombination spectroscopy on a diagnostic hydrogen beam—Measuring impurity rotation and radial electric field at the tokamak TEXTOR," J. Phys. B: At., Mol. Opt. Phys. **43**, 144015 (2010).
[3]E. L. Berezovskij *et al.*, "Local ion temperature measurements from Doppler broadening of hydrogen lines using a fast atomic beam," Nucl. Fusion **25**, 1495 (1985).
[4]E. S. Marmar *et al.*, "Diagnostic neutral beam and active spectroscopy requirements for the Alcator C-Mod tokamak (invited)," Rev. Sci. Instrum. **68**, 265 (1997).
[5]M. G. von Hellermann *et al.*, "Active beam spectroscopy for ITER," Nucl. Instrum. Methods Phys. Res., Sect. A **623**, 720 (2010).
[6]Y. I. Belchenko *et al.*, "Studies of ion and neutral beam physics and technology at the Budker Institute of Nuclear Physics, SB RAS," Phys.-Usp. **61**, 531 (2018).
[7]P. P. Deichuli *et al.*, "Long-pulse arc-discharge plasma source with cold cathode for diagnostic neutral beam injector," Rev. Sci. Instrum. **79**, 02C106 (2008).
[8]H. Gota *et al.*, "Formation of hot, stable, long-lived field-reversed configuration plasmas on the C-2W device," Nucl. Fusion **59**, 112009 (2019).
[9]P. P. Deichuli *et al.*, "Low energy, high power hydrogen neutral beam for plasma heating," Rev. Sci. Instrum. **86**, 113509 (2015).
[10]J. E. Boers, "A digital computer program for the simulation of positive or negative particle beams on a pc," in *Proceedings of International Conference Partic. Accel.* (IEEE, 1993), Vol. 1, p. 327.
[11]V. I. Davydenko *et al.*, "Radial electric field measurement in a tokamak by the injection of a pulsed neutral beam," Plasma Phys. Controlled Fusion **36**, 1805 (1994).
[12]R. Uhlemann *et al.*, "Hydrogen and deuterium ion species mix and injected neutral beam power fractions of the TEXTOR–PINIs for 20–60 kV determined by Doppler shift spectroscopy," Rev. Sci. Instrum. **64**, 974 (1993).
[13]M. Nations *et al.*, "Measurements of impurity ion temperature and velocity distributions via active charge-exchange recombination spectroscopy in C-2W," Rev. Sci. Instrum. **92**, 053512 (2021).
[14]R. S. Marshall *et al.*, "Upgraded main ion charge exchange recombination spectroscopy on the C-2W field reversed configuration (FRC) plasma," Rev. Sci. Instrum. **93**, 103542 (2022).

26 June 2024 06:54:28

© Author(s) 2024